Crack sealing and damage recovery monitoring of a concrete healing system using embedded piezoelectric transducers

Eleni Tsangouri[1,3], Grigorios Karaiskos[2], Dimitrios G Aggelis[1], Arnaud Deraemaeker[2] and Danny Van Hemelrijck[1]

[1] Vrije Universiteit Brussel (VUB), Department of Mechanics of Materials of Constructions (MeMC) Belgium

[2] Universite Libre de Bruxelles (ULB)-Building, Architecture and Town Planning (BATir) Belgium

[3] SIM vzw, Belgium

Corresponding author: Eleni Tsangouri, Vrije Universiteit Brussel (VUB), Department of Mechanics of Materials of Constructions (MeMC), Pleinlaan 2, 1050 Brussels, Belgium and SIM vzw, Technologiepark 935, BE-9052 Zwijnaarde, Belgium.
Email: etsangou@vub.ac.be

Abstract
The autonomous healing performance of concrete is experimentally verified by applying a technique based on the ultrasonic pulse velocity method using embedded piezoelectric transducers. Crack opening which deteriorates the mechanical capacity of concrete infrastructure is traditionally studied by different monitoring techniques that adequately provide a direct estimation of damage. Conversely in this research, an ultrasonic pulse velocity method is applied in order to monitor the crack closure and sealing of small-scale concrete beam elements. Short glass capsules filled with healing adhesive break due to crack formation and release that healing additives which fill the crack void and reset the element continuity. The damage index based on the early part of the wave arrival observes any emitted signal shape differentiation indicating the crack formation and development under two-cycle three-point-bending loading tests (in the first cycle, the crack forms and healing release take place and consequently after few hours of curing and crack reset the beam is reloaded leading to crack reopening).

Keywords
Autonomous, healing, concrete, fracture, encapsulation, SMAG, transducers

Introduction

Autonomous healing of construction materials using embedded capsules filled with healing agent [1], appears a breakthrough of recent research. Even in the case of vulnerable and time-limited concrete structures, new healing technologies promise service life extension when tubular capsules, filled with healing adherent, are placed a priori at the susceptible to cracking area. Cracks are inevitably formed and deteriorate concrete mechanical performance. As fracture damage occurs, crack discontinuity traverses the embedded capsules and enforces their rupture leading to healing agent release into the cracked void and activation of the recovery healing process. In the last decade, different research groups establish several concrete self-healing (SH) approaches that aim either to maintain or to restore material durability and previous consistency. Healing is mainly assessed by mechanical features regain though a validated observation requires visual inspection of damage recovery. However, the compact morphology of concrete elements prevents the monitoring of the crack volume sealing process.

At laboratory scale, X-ray radiography and tomography are commonly applied to visualise the release of encapsulated agent. The main drawback of the aforementioned penetrating radiation techniques is the limitation at the sample dimensions that lead to the destructive removal of the area of interest from the total element only after testing. Apparently, the fundamental understanding and systematic observation of cracked plane sealing and recovery demands a continuous monitoring method that detects and evaluates the healing activity. In this direction, the inspection of healing efficiency by low-cost piezoelectric transducers embedded into concrete elements is presented.

The ultrasonic pulse velocity technique using embedded piezoelectric transducers

Traditional structural ultrasound monitoring techniques operate inadequately in the case of in-situ concrete crack observations. The massive structural concrete elements suffer from multi-scaled cracks that cannot be detected by transducers attached to the material surface since their application requires a coupling agent and flat surface pre-treatment and additionally, lacks of flexibility in the transducers arrangement. Concerning the complex fracture process of crack opening and healing closure in concrete, an ultrasound detective technique that locally observes fracture is required. Particularly, the fracture recovery by a priori embedded healing chemical additives into the damaged region demands a technique sensitive enough to detect any modification in the internal concrete structure. On that direction, a promising alternative appears when the external transducers are replaced by low-cost piezoelectric transducers embedded in the concrete structures, following the Smart Aggregates (SMAG) concept initially developed at the University of Houston and recently deployed in the Civil Engineering Laboratory at ULB-BATir (Figure 1) [2-3].

A high voltage short rectangular wave (typically 800V with a pulse width of 2.5 μs) is generated in a computer system and delivered to the SMAG transmitter. Then, a wide band compressive wave (P-wave) is released that travels in all directions through concrete and is picked up by the available SMAG receiver(s). The received wave is filtered and preamplified before reaching a Data Acquisition system (DAQ) [4] in which the captured signal is properly post-processed in order to build a damage indicator representative of the damage evolution in the direct path between the transmitter and the receiver(s). The SMAG transducers consist of a low-cost flat piezoceramic PZT patch (Figure 1-a) of approximate size 12 mm*12 mm*0,2 mm. The electrical signals are transmitted to and from the transducer through electrical wires which are attached on both faces of the PZT patch (Figure 1-b). Then the patch is properly wrapped in a waterproof coating (Figure 1-c,d), in order to avoid any possible capacitive coupling between the transducers. As the PZT patch is very fragile, the waterproof layer provides additional mechanical protection. A thin layer of conductive paint is finally applied to provide efficient electromagnetic shielding (Figure 1-e). Consequently, the SMAG transducers can be placed in any place within the concrete structure without the use of coupling agent, thus facilitating the monitoring design.

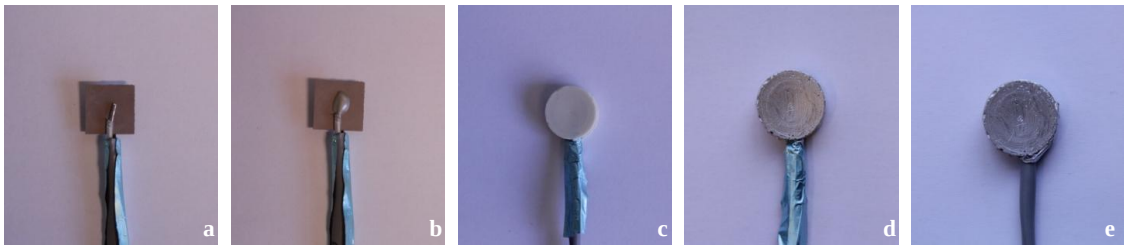

Figure 1: SMAG transducer manufacturing process (a-e).

Autonomous damage recovery by embedding into concrete encapsulated healing material

Imitating the healing mechanisms of natural organisms, materials science has developed autonomous reparation systems that aim to extend the service life of the constructions. The pioneering research of White et al. on encapsulated healing agent into

polymers provides for the first time mechanical recovery of cracked area as soon as the capsules rupture and the healing agent is released filling the damaged plane [1]. A decade after, several healing systems (based on bacterial precipitation, agent micro-encapsulation, agent embedment into hollow tubes, autogenic healing, etc.) ensure regain of strength and stiffness under different loading conditions (thermal damage, micro-cracking, fatigue, corrosion, etc.) on constructive materials such as metals, asphalt, ceramics, polymeric and cementitious composites [5].

In the case of concrete, wide cracking formed by extensive microcracks spread in the whole volume of structures requires great amount of healing material carried and released at the fractured area. Recently, at Magnel Laboratory of Ghent University, an innovative healing mechanism has been generated and it is able to heal concrete cracks up to 0,3 mm wide [6]. In fact, oblong hollow glass tubes are employed to carry a two-component expansive polyurethane based healing agent (adhesive and accelerator). During casting, the tubular capsules are placed in couples at different locations into the material where damage is expected. The crack propagation transverses the capsules and break the brittle glass tubes concurrenlty leading to healing agent release. The two adhesive components fill the crack void and by completing the curing time (24 hours) reset the consistency of concrete material. The efficiency of the aforementioned healing mechanism is being investigated under different loading conditions and using plethora of experimental techniques [7].

Up to now, previous research established a method to detect the tubular capsules breakage during the crack formation and identify the conditions under which healing activation occurs [8]. In parallel, the fracture response of concrete beam specimens tested under two-step pre-crack controlled bending tests (two cycles of loading: (a) crack formation-release of healing agent after capsules breakage (b) crack re-formation after curing) indicates partial regain of strength and stiffness after healing. Acoustic (Acoustic Emission) and optical (Digital Image Correlation) techniques monitor the crack evolution after healing [9-10]. Although, the significant findings regarding the fracture evolution after healing, the sealing and the local consistency restoration of the crack is not recorded and thoroughly determined. The subsequent experimental setting purports to clarify that occurrence.

Description of the experimental setup

Healing configuration

Plain concrete beams are prepared, cast into wooden molds and eventually fractured under three-point bending loading. The concrete mix proportions are given in Table 1. The specimen geometry and loading configuration is chosen to provide straightforward opening mode of fracture in concrete. Following the Rilem Technical Report FMC−50 regarding the fracture mechanisms in concrete, prismatic beams 840 mm long, 100 mm wide and 100 mm high are prepared [11]. At the middle section of the beam, a 10 mm high pre-notch is inserted by means of teflon strip. As pin load occurs in the middle of the beam, pre-crack serves to activate fracture and guide the crack propagation up to the top of the specimen.

Before concrete casting, the suspectible to cracking region above the pre-crack, is filled by the fragile glass tubes sizing 50 mm long and with inner diameter of 3 mm. The capsules, as shown in Figure 2, are placed in couples (attached on a low-stiffness plastic cord that sets their fixed position) and serve as carriers of the two-component polyurethane-based healing agent. The healing material is sealed and stored into the capsules until the moment that crack deformation causes the carriers rupture and

Table 1: Concrete mix proportion.

Material	Content (/m^3)
Sand 0/4	670 kg
Gravel 2/8	490 kg
Gravel 8/16	790 kg
Cement CEM I 52.5 N	300 kg
Water	150 kg

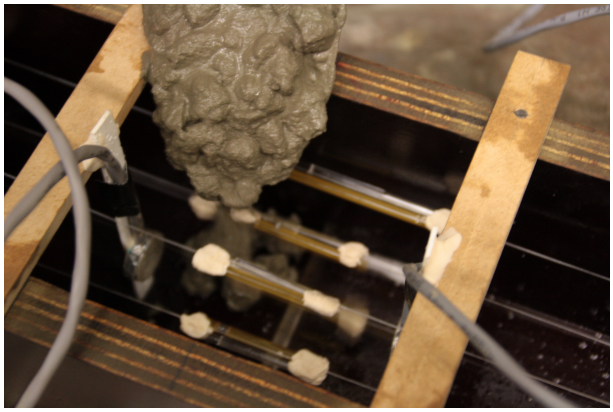

Figure 2: Casting process: embedded glass capsules and SMAG transducers are placed above and at both sides of the pre-cracked beam section respectively.

the agent is released into the fractured plane. At that time, the two agent components get in contact and healing polymerization mechanism is activated. Essential restoration process is considered complete 24 hours after cracking (curing period).

Two bending test cycles are performed. An Instron electromechanical frame applies deflection at the middle section of the beam (span of bending is fixed at 800 mm) and a Crack Mouth Opening Displacement (CMOD) device is attached at both sides of the pre-notched groove to measure the crack opening. At first, the undamaged concrete beam is loaded under deflection control (displacement rate 0,04 mm/min) up to crack opening of 0,3 mm. At that stage, crack formation ruptures the capsules and agent release activates the healing process. After the 24 hours curing period, the beams are retested under the same loading conditions. At that second stage, the recovery due to healing of the cracked region is evaluated by means of strength and stiffness regain.

SMAGs transducers setting

SMAG transducers P-wave emission was efficiently applied in the past to detect crack initiation and propagation in several concrete test settings [12-13]. In practice, the travelling time of the P-wave defines the mechanical condition of the material standing between the transmission and receiving locations. Considering as early arrival the direct wave contribution following the path between the transmitter and receiver SMAG transducers, the wave scattering due to material obstacles is eliminated and a linear relation between velocity and arrival time is established. Both travelling time and propagation velocity inclusively indicate the fracture evolution. Particularly, the decay or growth of several wave feature values are proportional to the degree of crack opening and closure respectively. For instance, SMAG transducers high sensitivity may locally track the damage by means of wave energy and amplitude drop and prospectively detect autonomous sealing by healing material insertion that provides wave features recovery.

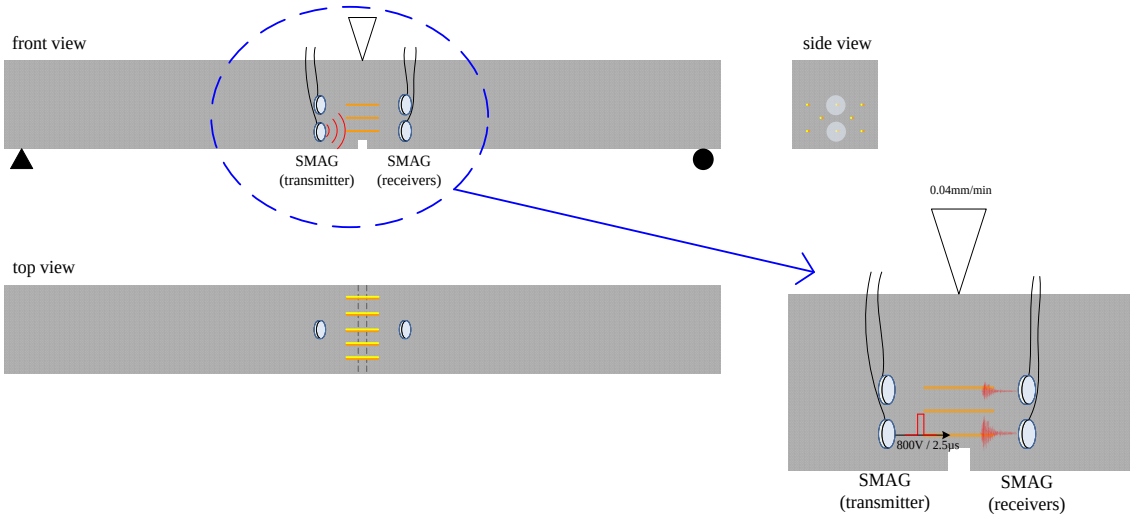

Figure 3: Concrete beam drawing: front/top and side view of SMAG configuration.

An overview of SMAG transducers monitoring system setting and the technical detailing are given in Figure 3. During testing, the emitted signals consequently form wavelengths short enough to be sensitive to fracture gaps or fillings, qualitatively determine the concrete health status by introducing a simple damage index, based on the early part of the measured waves.

The damage index (d.i) is defined by the Root Mean Square Deviation (RMSD) value between two signals captured at the healthy stage (undamaged concrete in our case) and over testing (loading-healing curing-reloading in our case) respectively. The damage index is computed in the time window corresponding to the first half-period of the healthy signal (shortest wave path affected only by material mechanical condition). The equation providing the d.i. is given in Figure 4 where x_o, x_j stand for the signal amplitudes on the healthy stage and a moment j during loading respectively, $(tp - tn)$ stands for the duration of the first half-period. A schematic representation of damage index variables is given as well in Figure 4.

By definition, the d.i. considers both the shift of the arrival time and the amplitude variations. Thus, any increase of the d.i. measured under bending deflection is indicative of crack formation and extension. On the other hand, any numerical restriction states crack sealing and recovery (since the damage dispersion is confined).

$$d.i.(j) = \sqrt{\frac{\int_{tn}^{tp} ((\mathrm{x_j(t)} - \mathrm{x_o(t)})^2 \, \mathrm{d}t}{\int_{tn}^{tp} \mathrm{x_o(t)}^2 \, \mathrm{d}t}} \qquad (1)$$

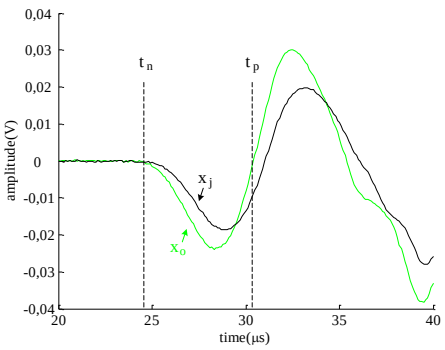

Figure 4: Damage index formula and early part signal drawing.

Results

Bending cycles evaluating healing efficiency: cases of study

In Figure 5 the load-crack opening curves of several beams series as obtained during both bending cycles are introduced. The continuous lining refers to the loading cycle of several series and respectively the dotted lines stand for the reloading cycle bending performance.

The analysis concerning the healing performance requires a normalized capsule breakage pattern. Acoustic Emission (AE) contributes to that direction by detecting the sound activity originated from the glass tube rupture. As recently presented in previous research [8], AE energy based analysis confirms the healing activation by capsule breakage as soon as crack forms and propagates across the concrete material. For the sake of completeness, the loading moments at which capsule breakage occurred are subsequently presented in Figure 5. It is observed that large number of capsule breakage events (affirming that all the embedded capsules ruptured) appeared during the crack formation and propagation stage of loading for all the specimens concerned in this study. Below, having proven the healing agent stimulation, the sealing and recovery performance is analytically investigated by the ultrasonic pulse velocity technique using embedded SMAGs.

Considering the healing performance, the concrete material tested is classified in three series presented in Figure 5. The modified features in each case is the healing agent characteristics/distribution and the height level of SMAG transducers. In detail:

Case A: reference-no healing activity

A concrete beam is prepared and four couples of empty glass capsules are embedded into according to the casting instructions above. Despite the absence of healing material that series aims to contribute as a reference measurement (healing activity is not expected). In parallel, both the main sources of fracture process (concrete cracking and capsule rupture) stand even in that case to ensure same loading conditions at all testing series. One pair of SMAG transducers is fixed at a height of 35 mm from the bottom of the beam.

Case B: partial damage recovery due to healing

A concrete beam is cast and four couples of glass capsules, filled by limited amount of inefficient healing agent, are placed into concrete. In this case, healing is activated and limited agent is released covering partly the damaged plane but still mechanical recovery is not achieved. A pair of SMAG transducers facing the crack is located 35 mm above the bottom of the beam.

Case C: healing performance monitored at different crack heights

Two concrete beams are cast and eight couples of glass capsules, filled by sufficient amount of healing agent, are embedded. The material setting is designed to provide sufficient damage recovery of the crack formed under bending. In the first beam, a pair of SMAG transducers is placed at a height of 35 mm from the bottom of the beam (case $C-1$) and in the second two pairs of SMAG transducers are embedded (case $C-2$) at different heights 20 and 50 mm from the bottom of the beam. During bending test, one of the SMAG transducers, located closer to the bottom of the beam is chosen to continuously

contribute as transmitter and the two SMAGs, standing at the other side of the pre-notched groove receive the signal propagated through the cracked plane. With the aforementioned transducers placement, the sealing of the crack and the mechanical performance regain is aimed to be monitored at different heights across the crack. A detailed drawing of the C-2 case, giving schematically a representative experimental setting, is shown in Figure 4.

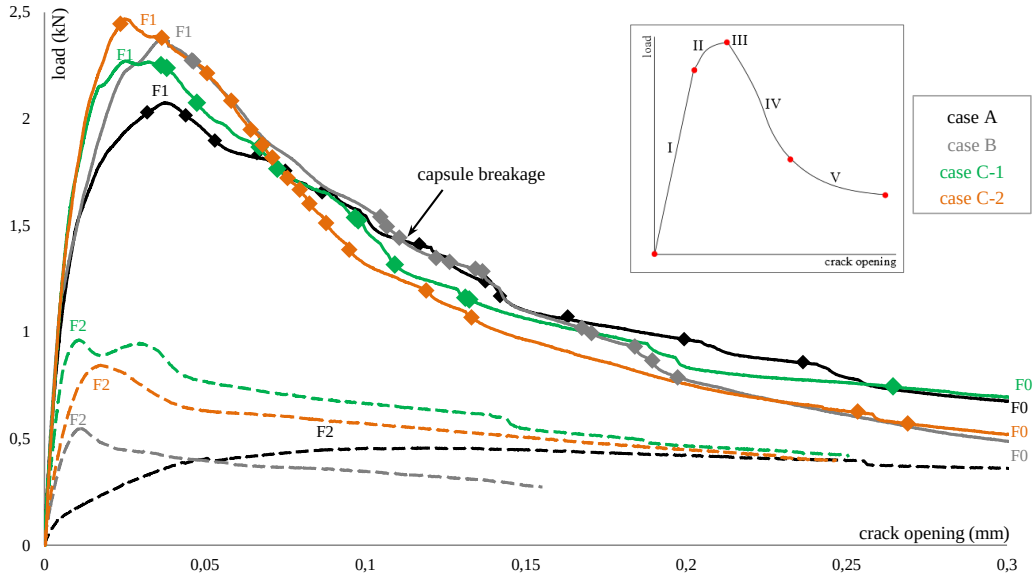

Figure 5: Two-cycle bending test: crack formation and reopening after healing agent curing. The moments of capsule breakage are given by marks. A drawing qualitatively indicating the cracking steps (I-V) is also provided.

Strength and stiffness regain

In Figure 5, the loading-crack opening graphs as obtained for the different cases analysed under two cycles of three-point bending tests are presented. The load and stiffness recovery at the second loading cycle (following the healing activation and curing of agent) are well established as indicators of healing efficiency [6]. With that approach, the ultimate load (both at loading and reloading stage) and the initial compliance are chosen to quantitatively evaluate the healing response in Table 2.

Table 2: Cases of study: healing configuration and evaluation as shown in Figure 3 [6]: strength regain=$\frac{F2-F0}{F1-F0}$ stiffness regain=$\frac{\frac{Fat40\%F2}{crackopeningat40\%F2}}{\frac{Fat40\%F}{crackopeningat40\%F}}$

cases	numbers of SMAG receivers	SMAG position from the bottom(mm)	strength regain* (%)	stiffness regain* (%)	healing performance
case A	1	35	0	0	reference
case B	1	35	0	40	partial healing
case C-1	1	35	36,5	88	healing
case C-2	2	25 and 50	21	45	healing

As shown at the two-cycle bending curves, during reloading, the damaged material of case A cannot withstand bending load greater than the load at the end of the first cycle, pointing the absence of any crack resistance. The reference material, as expected since healing is not considered, lacks the initial elastic response of quasi-brittle concrete nature providing no evidence

of stiffness recovery. Regarding the reloading performance of case B beam, partial stiffness regain is observed. In comparison to case A, the initial linear inclination is recovered up to 40% of the loading cycle compliance. Despite this, strength regain is not achieved since the peak load at the reloading cycle was not able to surpass the load at the end of the loading bending cycle. The limited amount of agent and the insufficient bonding efficiency of the healing material is confirmed. Noticeable mechanical recovery is obtained in the cases C, in which strength and stiffness restore is measured up to $21-36{,}5\%$ and $45-88\%$ for case $C-2$ and $C-1$ respectively. As shown in Figure 5, the initial compliance is well reset after healing agent curing and the loading capacity obtained at the second cycle overcomes the final load of the loading bending cycle for both beams.

Regrettably, the insufficient recovery of opened crack cannot be shown in the global overview of the bending response. The only evidence of healing activation is the location of capsule breakages by means of AE energy analysis, as introduced in previous paragraph. According to the marks in Figure 5, for all the cases of the analysis the capsules break releasing the healing agent at several post-peak loading stages. The effect on cracking response and the contribution of the released healing material to the mechanical performance is further investigated in detail using the ultrasonic pulse velocity technique by embedded SMAG transducers.

Evolution of wave velocity at both loading stages

The travelling time of compressional P-wave into concrete over a known distance contributes further on that research since it provides the mechanical condition of the element[14−15]. As introduced, the fixed location of SMAG transducers ensures determinate distance between the points of wave transmission and reception. The emergence of a macro-crack decreases significantly the wave propagation time since the released compressive wave is scattered and dispersed at the crack front plane before reaching the received transducer. It should be pointed that the bending fracture intensely affects the time delay relatively to microvoids, aggregates and glass tubes embedded into the concrete specimens. Considering the analysed concrete beams, wave velocity gradual decline is observed during bending in all three cases. At the loading cycle, the travelling time remains constant until the crack formation providing a stable wave velocity presented for each case on the first column in Figure 6. Beyond crack release load, the time delay almost linearly increases until the end of bending. Consequently, as the crack propagates, the wave velocity is significantly reduced towards the values given for each beam series on the second columns in Figure 6. At the bottom of Figure 6 plots of the velocity evolution during loading/reloading are given for the sake of completeness.

The wave velocity deterioration is well-studied in the past and linked to the crack fracture in concrete [13, 16-17]. In reverse, diffuse ultrasound on autogenous healed concrete correlates the crack width reduction after healing to the arrival time of the signal maximum energy [18]. The novelty of the current study is the monitoring of fracture recovery due to autonomous sealing by means of wave velocity reset. In detail, the third columns in Figure 6 presents the wave velocity as measured at the beginning of the reloading cycle. As expected, in the case of reference material, the absence of healing prospect, the velocity is measured at the same values as previously (velocity recovery at 0%). On the contrary, the wave velocity is slightly regained in the case of the beam with partial stiffness recovery by insufficient healing. As shown in case B of Figure 6, the velocity measured after agent curing is recovered by 33,3%.

Further, the efficient healing in case C as obtained at the loading response, discussed at the previous paragraph, is evident even by

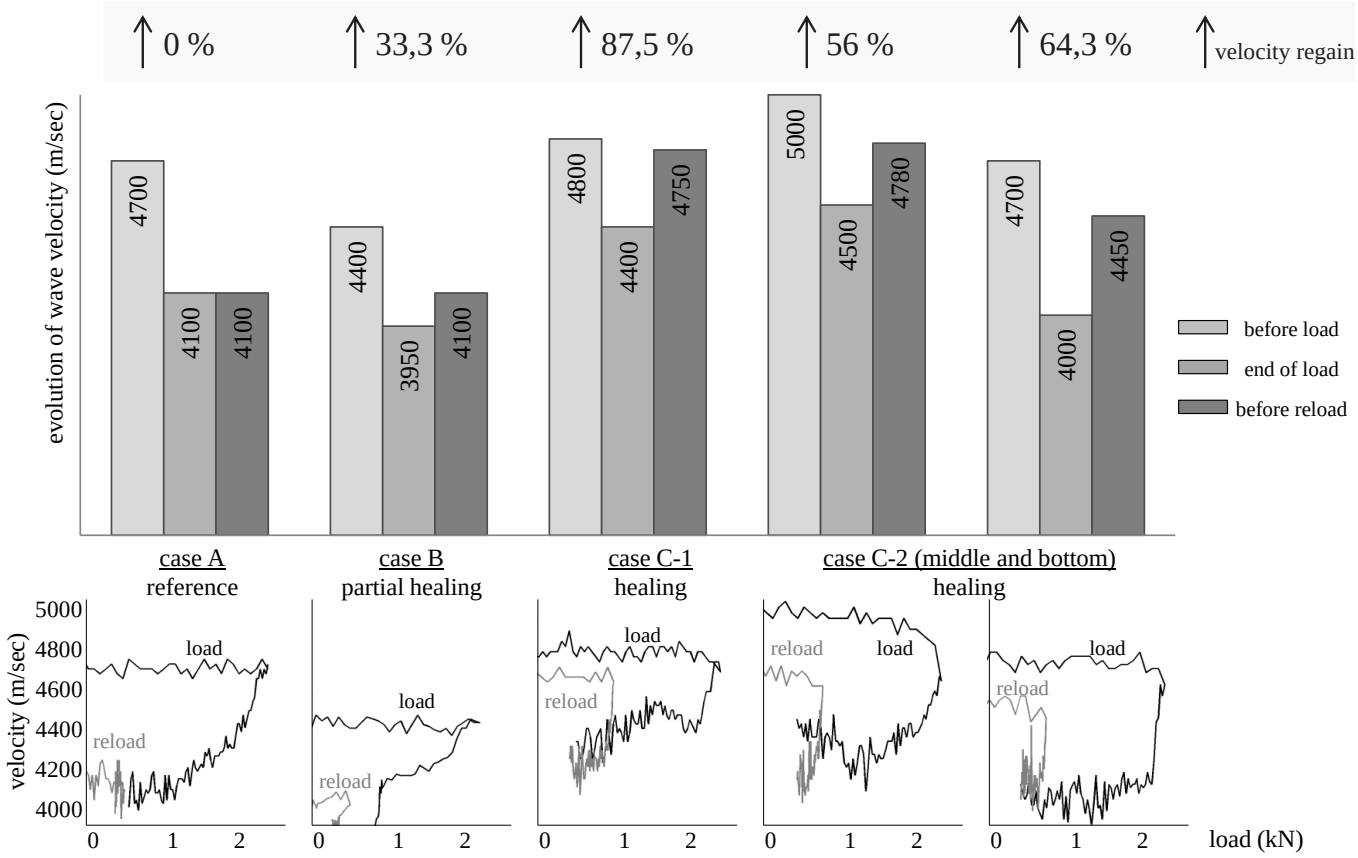

Figure 6: Wave velocity evolution at both cycles of loading (case C-2 results are given for both SMAG transducers receivers standing 25 and 50 mm above the bottom of the beam respectively) where velocity regain=$\frac{velocity before reloading - velocity at the end of loading}{velocity before loading - velocity at the end of loading}$ respective to strength and stiffness regain defined above in Table 2.

wave velocity measurements. The released healing agent fills the crack and covers the opened volume restricting the distortion effects on the early part of the propagated wave. The significantly shorter travelling time leads to wave velocity rest up to 87,5% after damage in case C-1. It is highlighted that even if the crack is fully filled, the velocity is not expected to be totally recovered to the initial value due to stiffness discrepancies between the concrete matrix and the healing agent as previously shown [19-20]. The great velocity recovery of case C−1 is correlated to the high stiffness restoration (88%) as obtained on the load response analysis (see Figure 5).

In case C−2, the allocation of the released healing agent at different heights of the beam is detected. More specifically, a slight difference in the wave velocity recovery might indicate the cracked regions in which healing performed better. However, definite finding cannot arise from the wave arrival time analysis. Further focus at several wave features (e.g. amplitude of received signal) and the crucial early part of the arrived signal may provide the state of fracture and efficiency of crack healing.

Evolution of the received signal amplitude at both loading stages

The bending deflection rate is chosen to comprehensively display the quasi-brittle cracking propagation, and simultaneously, to enable the ultrasonic pulse velocity technique using embedded SMAGs to continually track the progressive damage. The gradual crack opening/closure/reopening is captured as the information carried at the early part of the signal that contains the contribution

of a direct wave between the SMAG transmitter and the SMAG receiver. The received signal amplitude evolution of the direct waveform is derived for the following vital cracking fracture steps (schematically represented by the drawing in Figure 5):

step I: The initial loading response is linear as elastic deformation of the beam occurs.

step II: The non-linear loading response indicates microcracking fracture on concrete. At critical load, localized damage is introduced and fracture zone around the pre-notch forms [21].

step III: Reaching the concrete strength, load drops and crack releases from the pre-notch as strain softening plasticity initiates.

step IV: The crack propagates further up to the top of the beam. The loading drops almost linearly suspended by limited crack arrest ahead of the glass capsules.

step V: The second part of the bilinear post-peak load drop occurs as the resistance to damage ceases and the crack gets wider.

In Figure 7, series of signal windows present the early part of the received signal as monitored at respective cracking steps (I-V) during both bending cycles for the three cases under study. Furthermore, in Figure 8, the information derived from the signal window above is normalized and associated to the load and crack opening evolution. For the sake of completeness, a schematic overview of wave velocity, concrete strength and stiffness regain for all three cases is shown as well.

As expected, the crack initially forms controlled by the same fracture mechanisms throughout the several beams thus the loading cycle signal response is nearly identically repeated. The first period amplitude received at the beginning of loading is progressively effeminate as crack widens. The amplitude range differentiates as soon as step II of loading occurs since concrete microcracking introduces attenuation and distortion effects. The degradation dominates as the strength of concrete is reached (step III) and the attenuation affects the early part of the overall signal shape. At the end of loading cycle the signal form is significantly modified and the amplitude is considerably decreased by a factor of 10 (step IV and V). The accomplished amplitude measured as cracking indicates the damage state before healing insertion. Therefore, cracking filling is confirmed since after curing of the released agent the signal amplitude is successfully recovered.

It is not so in the case of reference beam (case A) where the signal recorded at the beginning of reloading cycle obtains an amplitude value equal to the loading final one. Furthermore,as shown in Figure 7 the signal strength remains immutable during reloading cycle evidencing the lack of mechanism that may provide resistance to crack reopening. On the contrary, a limited amplitude recovery is monitored in the case B of the analysis, in which the signal amplitude at beginning of reloading shows an increase of more than 10% relatively to the damaged state at the end of loading. The amplitude partial regain is correlated to the stiffness restoration but the absence of strength recovery is evident by the invariable wave shape throughout reloading test (Figure 7).

Both amplitude initial restore and signal shape variation during bending is monitored in the case C reloading tests. As demonstrated in the early part of the signals of Figure 7, the amplitude value is well regained after agent curing and sealing of the

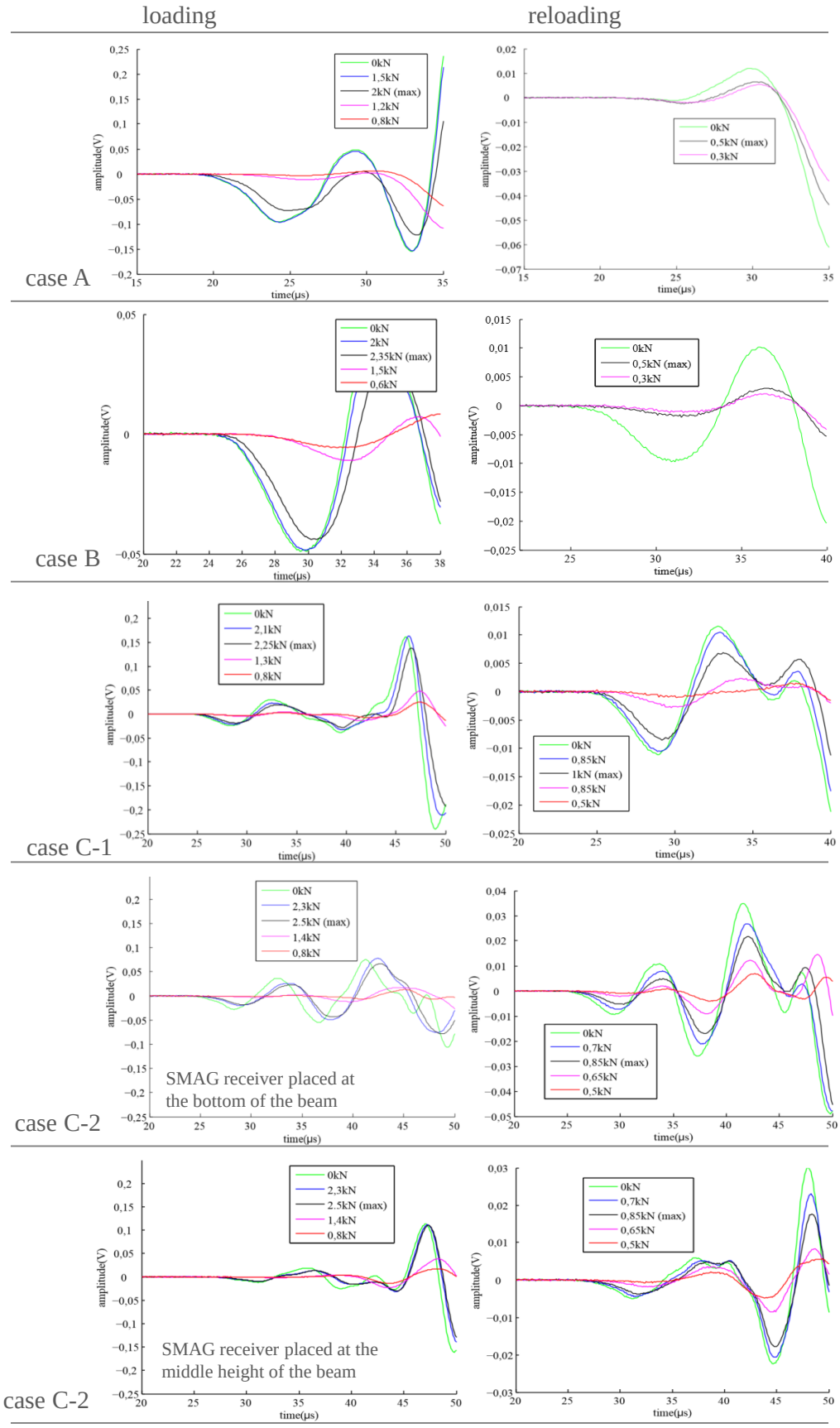

Figure 7: Early part of wave as received at different stages of loading/reloading cycles.

damaged concrete zone. Numerically, the signal amplitude is reverted up to 50% relative to the loading bending cycle. Furthermore, restored resistance to damage is displayed by the waveform shape spread as crack reopens. It is observed, similar to the loading case damage propagation, that the signal loses its initial magnitude (degradation) and morphology (widening and flattening) as crack traverses the healed region.

Respectively, in Figure 8, the signal amplitude as obtained at the beginning of the loading cycle (step I of analysis) reflects the healthiest conditions under investigation and based on that an amplitude normalization calculated at several loading steps is presented. For that reason, the normalized value chosen at the start of loading is equal to unity and after crack propagation the normalized amplitude is decreased up to 0,1 at step V of loading cycle (similar deterioration for all the beams). On the other hand, amplitude recovery is well noted as soon as healing agent curing occurs. As shown in Figure 8, the amplitude is increased up to 60% in the case C-2 as measured by the SMAG transducer standing in the middle height of the beam. The least amplitude restoration is calculated for the case B of partial healing. Lastly, a correlation between the amplitude regain and the stiffness and P-wave velocity restore is observed. It is shown that the waveform amplitude as measured before reloading can provide a good indicator of wave velocity and stiffness recovery due to healing. As expected the amplitude at the early part of the signal is sensitive to the concrete rigidity and damage existence.

Furthermore, the amplitude normalization (based on the healthy status) applied once again at step II of crack formation during both cycles of bending correlates to the absence of strength regain as measured at the loading-crack opening curves. As anticipated, the mechanical recovery is well captured in case C amplitude observations. On the other hand, it is worth pointing the lack of amplitude value recovery in the case B of partial healing. At the bending step of crack reopening the amplitude deteriorates further after initial damage.

Evaluation of damage index at both loading stages

On an integrated approach, the damage evolution, calculated by the normalized damage index plotted as a function of the applied load aims to provide a comprehensive view of cracking process during testing. The d.i. distribution is plotted in Figure 9 for the several healing cases.

At loading cycle, d.i. evolves similarly for all three cases recording the five steps of bending fracture. The initial elastic response of concrete provides almost zero d.i. values (step I of fracture). The deviation from zero, associated with certain level of noise in the signal, is minimal and can be negligible. The introduction of microcracks and fracture zone formation differentiates the d.i. from zero values as step II of cracking occurs up to the strength of concrete (step III). As crack propagates till the top of the beam (step IV) the d.i. value increases significantly reaching the unitary level and forming a plateau as crack widens (step V). At the end of loading cycle,the great d.i. indicates that the opening of crack disturbs (almost prevents) the wave propagation and scatters the signal transmitted.

In case C-2, there is a great differentiation regarding the initiating point of the first cycle crack fracture. As shown in Figure 9, the d.i. appears and deviates from zero earlier as calculated at the bottom of the beam (SMAG receiver stands at a height of 25 mm from the bottom of the beam) than the one measured at a higher level of the beam (the second SMAG receiver transducer is fixed 50 mm above the specimen). Therefore, the d.i. is able to promptly detect crack formation at the pre-notched region of the

beam. Actually, the d.i. deviation from zero as measured at the lower level of the beam appears earlier than the deviation from linearity in the loading graphs of Figure 5. It is shown that the d.i. is sensitive to the preliminary manifestation of cracking and detects microcracking initial damage.

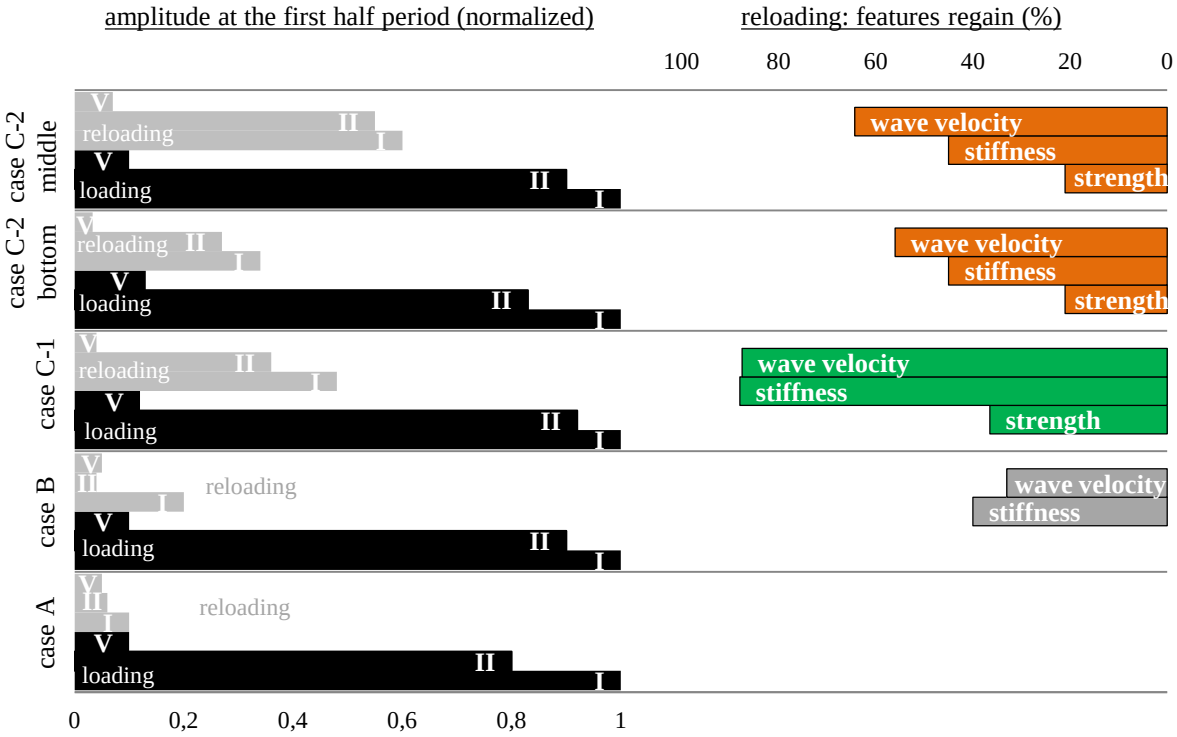

Figure 8: Early half-period amplitude evolution during both cycles of loading correlated to the mechanical recovery.

At reloading cycle, the d.i. evolution reveals the efficiency of healing process. Once again, the reference case A shows no damage recovery by giving unitary d.i. values during the whole reloading test. Limited reduction of d.i. value is obtained in the case B of the analysis, in which at the beginning of reloading cycle, the normalized d.i. is equal to 0,85. However, significant decrease of d.i. after healing agent curing occurs in the case C−1 and C−2 as the indicator initial value is measured less than 0,6 for both cases. Furthermore in case C−2, it is shown that the crack sealing by means of released healing agent can perform better at the damaged area with limited crack opening at the middle height of the beam compared to partial d.i. regain (more than 0,7) obtained at the bottom of the beam. It is concluded that the widely opened areas of the crack cannot be easily filled by healing material and sufficient restore their mechanical characteristics (both stiffness and strength). For the first time, a testing setting yields information on crucial areas of the healing material, by monitoring the wave propagation through damage in different locations.

Discussion-early part sensitivity to damage

Ultrasonic monitoring of damage evolution by SMAG transducers emerges as a key tool in the study of healing efficiency in concrete. The wave velocity of the transmitted signal as received by SMAG transducers at the healthy and healing state indicates

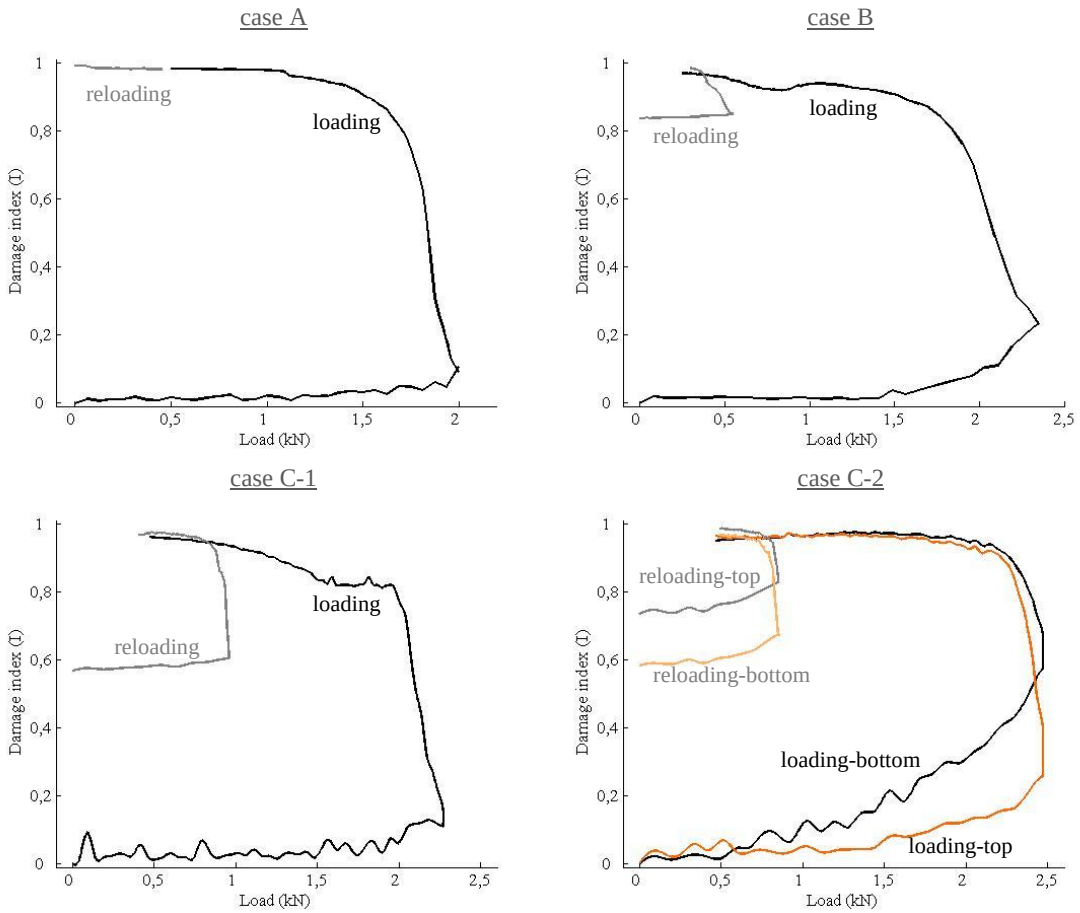

Figure 9: Damage index of loading and reloading cycles as assessed for all three cases of study.

mechanical recovery providing a preliminary exploration on the potentials of the technique.

The signal deterioration at the damaged state should be cautiously considered since wide crack formation leads to amplitude decrease up to the noise levels and thus arrival time misperceptions. Instead, the damage index continually merges the arrival time and amplitude information providing an integrated monitoring of crack evolution during testing. By calculating the modification of the early part of the signal received as crack forms, opens and reopens after healing, the d.i. seems to be very sensitive to any cracking variation. The shape and magnitude of the received signal, attain significant recovery as soon as sealing of the damaged area has occurred. For instance, in Figure 10, the early part of the two signals transmitted through a damaged and a healing recovered area as received by a SMAG transducer are placed together. The amplitude of the signal captured after released healing agent curing is considerably greater than the one captured before healing activation. In parallel, the overall shape of the signal early part resets its initial healthy density compared to the spread signal captured at the damaged state.

Conclusions

Until today, ultrasounic pulse velocity technique using SMAGs seems to be a practical, cheap and efficient technique to assess concrete curing conditions [22] and damage that overcomes the experimental limitations of traditional ultrasonic techniques. For the first time, SMAG transducers monitoring is successfully applied to evaluate the inverse fracture process: crack closure,

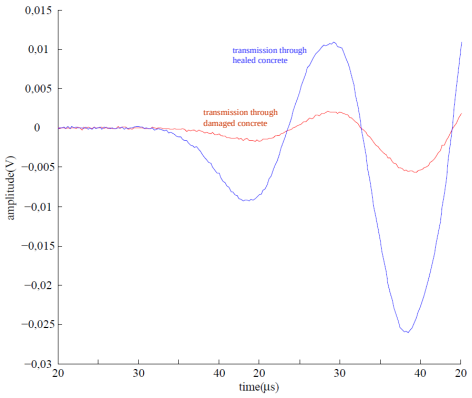

Figure 10: Detail of early part of signal indicative of sealing recovery.

sealing and recovery of concrete cracks up to 0,3 mm wide. The controlled pre-cracked three point bending setup forms damage propagating across the height of a small-size beam. SMAG transducers continuously monitor the crack evolution and the several signal features (P-wave velocity, waveform early part amplitude range, signal shape morphology) provide a respective damage indicator. By placing pairs of SMAG receiver-transmitter transducers at different height levels on both sides of the crack plane, the areas where healing agent is well released are detected. Evaluating the test configuration it should be pointed that the crack control by pre-cracking certainly serves to the transducers positioning close to the crack propagation zone. In cases of prospective more realistic concrete tests, where multiple cracking is expected or the cracks location and interaction is not known, SMAG monitoring transducers should be sophistically and strategically placed. Another topic of discussion is the attenuation effect on the propagated wave. In this case, attenuation does not prevent wave transmission and reception by SMAG. In case of longer distances between the transducers are applied excessive attenuation could be tackled with by adjusting the voltage input at the pulser.

Acknowledgements

The research described in this paper has been performed in the frame of the SIM program on Engineered Self-Healing Materials (SHE). The authors are grateful to SIM (Strategic Initiative Materials Flanders) and FNRS (Fonds de la Recherche Scientifique) for providing financial support.

References

[1] White S, Sottos N, Geubelle P, Moore J and Kessler S. Autonomic healing of polymer composites. Nature 2001; 409 (6822): 794-7970.

[2] Song G, Gu H and Mo YL. Smart aggregates: multi-functional sensors for concrete structures- a tutorial and a review. Smart Materials and Structures 2008; 17 (3)

[3] Gu H, Song G, Dhonde H, Mo YL and Yan S. Concrete early-age strength monitoring using embedded piezoelectric transducers. Smart Materials and Structures 2006; 15 (6): 1837-45.

[4] Reinhardt HW, Grosse CU. Continuous monitoring of setting and hardening of mortar and concrete. Construction and Building Materials 2004, vol. 18, issue 3: 145-154.

[5] SK Ghosh. Self-healing Materials: Fundamentals, Design Stategies, and Applications. Wiley-vch, 2008, p. 291.

[6] K. Van Tittelboom. Self-healing concrete through incorporation of encapsulated bacteria- or polymer-based healing agents. PhD Thesis, Department of Structural Engineering, Ghent University, 2012.

[7] Van Tittelboom K, De Belie N, Zhang P and Wittmann FH. Self-healing of cracks in concrete. In: International Workshop (ASMES)2011: Basic research on concrete and applications, Freiburg, Germany, pp. 303-314.

[8] Tsangouri E, Aggelis DG, Van Tittelboom K, De Belie N and Van Hemelrijck D. Detecting the Activation of a Self-Healing Mechanism in Concrete by Acoustic Emission and Digital Image Correlation. The Scientific World Journal 2013; Article ID: 424560.

[9] Tsangouri E, Van Tittelboom K, Van Hemelrijck D and De Belie N. Visualization of the healing process on reinforced concrete beams by application of Digital Image Correlation. In: 6th International Conference on High-Performance Structures and Materials, New Forest, UK, 2012, pp 1-12.

[10] Van Tittelboom K, Tsangouri E, Van Hemelrijck D and De Belie N. The efficiency of self-healing concrete using more realistic manufacturing procedures and crack patterns. accepted to be published at Cement and Concrete Composites 2014.

[11] RILEM TC-50-FCM, Determination of fracture energy of mortar and concrete by means of three- point bend tests on notched beams. Materials and Structures 1985; 18 (106): 285-290.

[12] Karaiskos G, Flawinne S, Sener JY and Deraemaeker A. Design and validation of embedded piezoelectric transducers for damage detection applications in concrete structures. In: 10th International Conference on Damage Assessment of Structures (DAMAS 2013), Dublin, Ireland, 2013.

[13] Dumoulin C, Karaiskos G and Deraemaeker A. Monitoring of crack propagation in reinforced concrete beams using embedded piezoelectric transducers.In: 8th International Conference on Fracture Mechanics of Concrete and Concrete Structures, Toledo, Spain, 2013.

[14] Zhang J and Li Z. Study on hydration process of early-age concrete using embedded active acoustic and non-contact complex resistivity methods. Construction and Building Materials 2013; 46: 183-192.

[15] Trtnik G, Kavcic F and Turk G. Prediction of concrete strength using ultrasonic pulse velocity and artificial neural networks. Ultrasonics 2009; 49: 53-60.

[16] Shokouhi P, Zoega A, Wiggenhauser H and Fischer G. Surface wave velocity-stress relationship in uniaxially loaded concrete. ACI Materials Journal 2012; 109 (2): 141-148.

[17] Quinn W, Kelly G and Barrett J. Development of an embedded wireless sensing system for the monitoring of concrete. Structural Health Monitoring 2012; 11(4): 381-392.

[18] In CW, Brett Holland R, Kim JY, Kurtis KE, Kahn LF and Jacobs LJ. Monitoring and evaluation of self-healing in concrete using diffuse ultrasound. NDT and E Int 2013; 57: 36-44.

[19] Aggelis DG and Shiotani T. Repair evaluation of concrete cracks using surface and through-transmission wave measurements. Cement and Concrete Composites 2007; 29: 700-711.

[20] Momoki S, Shiotani T, Kian Chai H, Aggelis DG and Kobayashi Y. Large-scale evaluation of concrete repair by three-dimensional elastic-wave-based visualization technique. Structural Health Monitoring 2013; 12: 240-251.

[21] Elices M, Guinea GV, Gomez J and Planas J. The cohesive zone model: advantages, limitations and challenges. Engineering Fracture Mechanics 2002; 69(2): 137-163.

[22] Dumoulin C, Karaiskos G, Carette J, Staquet S and Deraemaeker A. Monitoring of the ultrasonic P-wave velocity in early-age concrete with embedded piezoelectric transducers. Smart Materials and Structures 2012; 21(4) DOI: 033001.